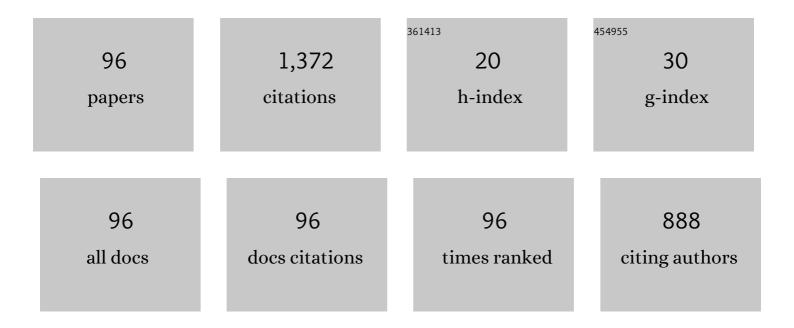
List of Publications by Year in descending order

Source: https://exaly.com/author-pdf/328873/publications.pdf Version: 2024-02-01



#	Article	IF	CITATIONS
1	Influence of ambient gas and its pressure on the laser-induced breakdown spectroscopy and the surface morphology of laser-ablated Cd. Applied Physics A: Materials Science and Processing, 2012, 107, 203-212.	2.3	79
2	Effect of ambient gas conditions on laser-induced copper plasma and surface morphology. Physica Scripta, 2012, 85, 015702.	2.5	69
3	Effect of dry and wet ambient environment on the pulsed laser ablation of titanium. Applied Surface Science, 2013, 270, 49-57.	6.1	60
4	Femtosecond laser-induced subwavelength ripples on Al, Si, CaF2 and CR-39. Nuclear Instruments & Methods in Physics Research B, 2012, 275, 1-6.	1.4	55
5	Effect of ambient environment on excimer laser induced micro and nano-structuring of stainless steel. Applied Surface Science, 2012, 261, 101-109.	6.1	37
6	Effect of laser irradiance on the surface morphology and laser induced plasma parameters of zinc. Laser and Particle Beams, 2014, 32, 119-128.	1.0	35
7	Effect of magnetic field on laser-induced breakdown spectroscopy of graphite plasma. Applied Physics B: Lasers and Optics, 2016, 122, 1.	2.2	35
8	SEM, AFM, EDX and XRD analysis of laser ablated Ti in nonreactive and reactive ambient environments. Surface and Coatings Technology, 2013, 235, 297-302.	4.8	32
9	Pulsed laser ablation of Germanium under vacuum and hydrogen environments at various fluences. Applied Surface Science, 2015, 344, 146-158.	6.1	31
10	Effect of ion irradiation on the surface, structural and mechanical properties of brass. Nuclear Instruments & Methods in Physics Research B, 2014, 325, 5-10.	1.4	29
11	Laser ablation of ion irradiated CR-39. Laser and Particle Beams, 2007, 25, 181-191.	1.0	28
12	Nanosecond pulsed laser ablation of brass in a dry and liquid-confined environment. Applied Physics A: Materials Science and Processing, 2013, 110, 389-395.	2.3	28
13	Morphological and spectroscopic characterization of laser-ablated tungsten at various laser irradiances. Applied Physics A: Materials Science and Processing, 2015, 119, 859-870.	2.3	28
14	Laser-induced breakdown spectroscopy of tantalum plasma. Physics of Plasmas, 2013, 20, .	1.9	27
15	Effect of laser fluence on surface, structural and mechanical properties of Zr after irradiation in the ambient environment of oxygen. European Physical Journal D, 2013, 67, 1.	1.3	27
16	Effect of liquid environment on the titanium surface modification by laser ablation. Applied Surface Science, 2017, 405, 298-307.	6.1	27
17	Effect of magnetic field on laser induced breakdown spectroscopy of zirconium dioxide (ZrO2) plasma. Optik, 2017, 140, 536-544.	2.9	23
18	Optical emission spectroscopy of magnetically confined laser induced vanadium pentoxide (V2O5) plasma. Physics of Plasmas, 2017, 24, 083112.	1.9	23

#	Article	IF	CITATIONS
19	Surface and structural modifications of titanium induced by various pulse energies of a femtosecond laser in liquid and dry environment. Applied Physics A: Materials Science and Processing, 2014, 114, 243-251.	2.3	21
20	The formation of nanodimensional structures on the surface of Tin exposed to femtosecond laser pulses in the ambient environment of ethanol. Applied Surface Science, 2014, 290, 53-58.	6.1	20
21	Pulsed laser ablation of Ni in vacuum and N <sub>2</sub> atmosphere at various fluences. Quantum Electronics, 2015, 45, 640-647.	1.0	20
22	Liquid assisted ablation of zirconium for the growth of LIPSS at varying pulse durations and pulse energies by femtosecond laser irradiation. Nuclear Instruments & Methods in Physics Research B, 2015, 349, 230-238.	1.4	19
23	Surface analysis correlated with the Raman measurements of a femtosecond laser irradiated Ca F2. Applied Surface Science, 2012, 258, 3178-3183.	6.1	18
24	Identification of non-thermal and thermal processes in femtosecond laser-ablated aluminum. Radiation Effects and Defects in Solids, 2013, 168, 902-911.	1.2	18
25	Mechanical behaviour of excimer laser irradiated polycrystalline zirconium. Physica Scripta, 2014, 89, 025703.	2.5	18
26	Laser irradiation effects on the surface, structural and mechanical properties of Al–Cu alloy 2024. Radiation Effects and Defects in Solids, 2014, 169, 144-156.	1.2	18
27	Effect of nature and pressure of ambient environments on the surface morphology, plasma parameters, hardness, and corrosion resistance of laser-irradiated Mg-alloy. Laser and Particle Beams, 2015, 33, 315-330.	1.0	17
28	Nonlinear absorption properties correlated with the surface and structural changes of ultra short pulse laser irradiated CR-39. Applied Physics A: Materials Science and Processing, 2010, 100, 1183-1189.	2.3	16
29	EFFECTS OF SUBSTRATE TEMPERATURE ON STRUCTURAL, OPTICAL AND SURFACE MORPHOLOGICAL PROPERTIES OF PULSED LASER DEPOSITED <font>ZnO</font> THIN FILMS. Surface Review and Letters, 2013, 20, 1350032.	1.1	15
30	Femtosecond laser induced nanostructuring of zirconium in liquid confined environment. Chinese Physics B, 2017, 26, 015204.	1.4	15
31	EFFECT OF SUBSTRATE TEMPERATURE ON THE GROWTH OF COPPER OXIDE THIN FILMS DEPOSITED BY PULSED LASER DEPOSITION TECHNIQUE. Surface Review and Letters, 2018, 25, 1850053.	1.1	15
32	Surface, structural, electrical and mechanical modifications of pulsed laser deposited ZrN thin films by implantation of MeV carbon ions. Nuclear Instruments & Methods in Physics Research B, 2019, 448, 61-69.	1.4	15
33	Laser-induced breakdown spectroscopy analysis of human deciduous teeth samples. Lasers in Medical Science, 2015, 30, 2233-2238.	2.1	14
34	Nanostructuring of zirconium by femtosecond laser irradiation in the ambient environment of air and ethanol. Optik, 2017, 134, 149-160.	2.9	14
35	3†MeV proton irradiation effects on surface, structural, field emission and electrical properties of brass. Nuclear Instruments & Methods in Physics Research B, 2018, 423, 7-15.	1.4	14
36	Magnetic field effect on plasma parameters and surface modification of laser-irradiated Cu-alloy. Laser and Particle Beams, 2018, 36, 261-275.	1.0	14

#	Article	IF	CITATIONS
37	Surface, electrical and mechanical modifications of PMMA after implantation with laser produced iron plasma ions. Nuclear Instruments & Methods in Physics Research B, 2016, 378, 1-7.	1.4	13
38	Femtosecond laser fluence based nanostructuring of W and Mo in ethanol. Physica B: Condensed Matter, 2017, 513, 48-57.	2.7	13
39	The role of laser fluence and ambient environments on femtosecond laser induced breakdown spectroscopy and on surface morphology of Mg and Zr. Journal of Applied Physics, 2019, 125, .	2.5	13
40	Nanosecond pulsed laser ablation of Ge investigated by employing photoacoustic deflection technique and SEM analysis. Physica B: Condensed Matter, 2016, 490, 31-41.	2.7	12
41	Spectroscopic and morphological investigation of laser ablated silicon at various laser fluences. Optik, 2018, 164, 186-200.	2.9	12
42	Laser-induced breakdown spectroscopy of aluminum plasma in the absence and presence of magnetic field. Applied Optics, 2019, 58, 1110.	1.8	12
43	The growth of nanoscale periodic and dot-like structures on the surface of stainless steel with femtosecond laser pulses in the dry and wet ambient environment. Applied Physics A: Materials Science and Processing, 2013, 113, 673-681.	2.3	11
44	Laser Induced Surface Morphology of Molybdenum Correlated with Breakdown Spectroscopy. Plasma Chemistry and Plasma Processing, 2017, 37, 287-304.	2.4	11
45	Femtosecond laser induced periodic surface structures for the enhancement of field emission properties of tungsten. Optical Materials Express, 2019, 9, 3183.	3.0	11
46	Identification of ultra-fast electronic and thermal processes during femtosecond laser ablation of Si. Applied Physics A: Materials Science and Processing, 2012, 109, 421-429.	2.3	10
47	Spectroscopic and morphological study of laser ablated Titanium. Optics and Spectroscopy (English) Tj ETQq1	1 0.784314 0.6	4 rgBT /Over
48	The role of spatial confinement for improvement of laser-induced Mg plasma parameters and growth of surface features. Applied Physics A: Materials Science and Processing, 2017, 123, 1.	2.3	10
49	Fluence-dependent sputtering yield measurement, surface morphology, crater depth, and hardness of laser-irradiated Zr in N <sub>2</sub> and Ne environments. Journal of the Optical Society of America B: Optical Physics, 2019, 36, 1945.	2.1	10
50	Spatial confinement effects on spectroscopic and morphological studies of nanosecond laser-ablated Zirconium. Optics and Laser Technology, 2017, 97, 60-70.	4.6	9
51	Investigation of field emission properties of laser irradiated tungsten. Applied Physics A: Materials Science and Processing, 2018, 124, 1.	2.3	9
52	Characterizing laser induced plasma and ablation of Mg-alloy in the presence and absence of magnetic field. Optik, 2018, 170, 353-367.	2.9	9
53	Study of Micro/Nano Structuring and Mechanical Properties of KrF Excimer Laser Irradiated Al for Aerospace Industry and Surface Engineering Applications. Materials, 2021, 14, 3671.	2.9	9
54	Atomic force microscopy and Raman scattering studies of femtosecond laser-induced nanohillocks on CR-39. Nuclear Instruments & Methods in Physics Research B, 2009, 267, 3606-3610.	1.4	8

#	Article	IF	CITATIONS
55	Surface and morphological features of laser-irradiated silicon under vacuum, nitrogen and ethanol. Applied Surface Science, 2015, 357, 2415-2425.	6.1	8
56	Modifications in surface, structural and mechanical properties of brass using laser induced Ni plasma as an ion source. AIP Advances, 2016, 6, .	1.3	8
57	Epitaxial thin-film growth of Ruddlesden–Popper-type Ba3Zr2O7 from a BaZrO3 target by pulsed laser deposition. Applied Physics A: Materials Science and Processing, 2016, 122, 1.	2.3	8
58	Growth of surface structures correlated with structural and mechanical modifications of brass by laser-induced Si plasma ions implantation. Applied Physics A: Materials Science and Processing, 2017, 123, 1.	2.3	8
59	Surface morphology correlated with sputtering yield measurements of laser-ablated iron. Laser and Particle Beams, 2018, 36, 427-441.	1.0	8
60	Morphological, elemental and hardness analysis of femtosecond laser irradiated Al targets. Optics and Laser Technology, 2018, 108, 107-115.	4.6	8
61	Laser sputtering of Zr under Ar and O2 environments explored by quartz crystal microbalance and SEM analysis. Laser and Particle Beams, 2019, 37, 128-140.	1.0	8
62	Evaluation and measurement of laser induced Zr-plasma parameters along with self-generated electric and magnetic fields under various pressures of Ar environment. Optik, 2021, 246, 167790.	2.9	8
63	Investigation of Energy and Density of Laser-Ablated Si and Ge Plasma Ions Along With Surface Modifications. IEEE Transactions on Plasma Science, 2020, 48, 4191-4203.	1.3	8
64	Pulse duration and environmental effects on the surface nanostructuring and mechanical properties of zinc during femtosecond laser irradiation. Journal of the Optical Society of America B: Optical Physics, 2020, 37, 2878.	2.1	8
65	Surface topography of ultrashort laser-irradiated CaF2. Radiation Effects and Defects in Solids, 2011, 166, 30-34.	1.2	7
66	Surface, structural and mechanical properties of zirconium ablated by KrF excimer laser radiation. Quantum Electronics, 2016, 46, 1015-1022.	1.0	7
67	Spectroscopic and morphological studies of laser ablated silver. Optik, 2016, 127, 5128-5134.	2.9	7
68	Study of variation in surface morphology, chemical composition, crystallinity and hardness of laser irradiated silver in dry and wet environments. Optics and Laser Technology, 2017, 92, 173-181.	4.6	7
69	Femtosecond laser ablation of Zn in air and ethanol: effect of fluence on the surface morphology, ablated area, ablation rate and hardness. Applied Physics A: Materials Science and Processing, 2021, 127, 1.	2.3	7
70	Energy and flux measurements of laser-induced silver plasma ions by using Faraday cup. Plasma Science and Technology, 2021, 23, 085510.	1.5	7
71	Atomic force microscopy, Raman spectroscopy and nonlinear absorption properties of femtosecond laser irradiated CR-39. Applied Physics A: Materials Science and Processing, 2010, 101, 551-554.	2.3	6
72	SEM and Raman spectroscopy analyses of laser-induced periodic surface structures grown by ethanol-assisted femtosecond laser ablation of chromium. Radiation Effects and Defects in Solids, 2015, 170, 414-428.	1.2	6

#	Article	IF	CITATIONS
73	The generation, detection and measurement of laser-induced carbon plasma ions and their implantation effects on brass substrate. Radiation Effects and Defects in Solids, 2016, 171, 565-582.	1.2	6
74	Effect of fluence and ambient environment on the surface and structural modification of femtosecond laser irradiated Ti. Chinese Physics B, 2016, 25, 018101.	1.4	6
75	Study the effects of nitrogen ion implantation on structural and mechanical properties of AA7075. Materials Research Express, 2018, 5, 076507.	1.6	6
76	Effect of excimer laser fluence on the surface structuring of Ti under vacuum condition. Journal of Laser Applications, 2014, 26, 022003.	1.7	5
77	Structural, morphological and optical properties of pulsed laser deposited ZnSe/ZnSeO <sub>3</sub> thin films. Materials Research Express, 2018, 5, 046404.	1.6	5
78	Sputtering yield measurements of laser ablated Mg-alloy correlated with surface, structural and mechanical modifications. Optik, 2020, 207, 163866.	2.9	5
79	Time of flight measurements of energy and density of laser induced Mg plasma ions and investigation of ablated surface morphology. Physics of Plasmas, 2021, 28, 013113.	1.9	5
80	Effect of Phosphorous Ion Implantation on the Surface, Crystal Structure, Mechanical, and Electrochemical Properties of Bioresorbable Magnesium for Biomedical Applications. Journal of Materials Engineering and Performance, 2022, 31, 7695-7704.	2.5	5
81	CARBON ION IRRADIATION EFFECTS ON PULSED LASER DEPOSITED TITANIUM NITRIDE THIN FILMS. Surface Review and Letters, 2015, 22, 1550020.	1.1	4
82	Laser induced surface structuring of Cu for enhancement of field emission properties. Materials Research Express, 2018, 5, 025029.	1.6	4
83	Measurement of characteristic parameters and self-generated electric and magnetic fields (SGEMFs) of laser-induced aluminum plasma. Applied Physics B: Lasers and Optics, 2021, 127, 1.	2.2	4
84	Surface and Structural Modifications of Tungsten by Laser Irradiation for Enhanced Electrochemical Corrosion Resistance. Journal of Materials Engineering and Performance, 2022, 31, 1904-1913.	2.5	3
85	Carbon ion irradiation effects on surface modifications and field emission properties of molybdenum. Applied Physics A: Materials Science and Processing, 2022, 128, .	2.3	3
86	The variation in surface morphology and hardness of human deciduous teeth samples after laser irradiation. Laser Physics, 2017, 27, 115601.	1.2	2
87	Laser induced surface and structural modification of germanium in liquid environments. Journal of Laser Applications, 2018, 30, 012005.	1.7	2
88	Evaluation of electron temperature and electron density of laser-ablated Zr plasma by Langmuir probe characterization and its correlation with surface modifications. Laser and Particle Beams, 2020, 38, 84-93.	1.0	2
89	Investigation and correlation between surface modifications and field emission properties of laser-induced silicon plasma ion irradiated stainless steel. Radiation Effects and Defects in Solids, 2022, 177, 706-726.	1.2	2
90	Effect of laser pulses on the surface and structural modification of ablated titanium in a liquid-confined environment. Radiation Effects and Defects in Solids, 2015, 170, 121-129.	1.2	1

#	Article	IF	CITATIONS
91	Investigation of number density, temperature, and kinetic energy of nanosecond laser-induced Zr plasma species for self-generated electric and magnetic fields in axial expansion of plume. Journal of the Optical Society of America B: Optical Physics, 2022, 39, 1986.	2.1	1
92	Effects of unmagnetized and magnetically confined laser induced copper plasma ions on the surface, optical, wetting, electrical and mechanical properties of PMMA. Nuclear Instruments & Methods in Physics Research B, 2022, 526, 39-50.	1.4	1
93	Structural Modifications of KrF Excimer Laser-Ablated Zirconium Correlated to the Surface and Mechanical Properties. , 0, , .		Ο
94	The Irradiance-Based Growth of Surface Structures Induced by Nanosecond Laser Pulses On Si and Ge and Their Correlation with Plasma Ion Kinetic Energies and Densities. Journal of Micro and Nano-Manufacturing, 2022, , .	0.7	0
95	Langmuir Probe Characterization of Spatially Confined Laser-Ablated Iron Plasma Along With Surface Modifications. IEEE Transactions on Plasma Science, 2022, 50, 1206-1217.	1.3	0
96	Langmuir probe characterization of spatially confined laser-induced Bismuth plasma. Optik, 2022, 266, 169566.	2.9	0